Loss of Cbl-PI3K interaction in mice prevents significant bone loss following ovariectomy

Naga Suresh Adapala[‡], **Danielle Holland[§]**, **Vanessa Piccuillo[‡]**, **Mary F. Barbe[§]**, **Wallace Y. Langdon[#]**, **Alexander Y. Tsygankov[**]**, **Joseph A. Lorenzo[‡‡]**, and **Archana Sanjay[‡,1]**

[‡]Department of Orthopaedic Surgery, University of Connecticut Health Center, Farmington Connecticut, USA 06032

[‡‡]Department of Medicine, University of Connecticut Health Center, Farmington Connecticut, USA 06032

[§]Department of Anatomy and Cell Biology, Temple University School of Medicine, Philadelphia Pennsylvania, USA 19140

[**]Department of Microbiology and Immunology, Temple University School of Medicine, Philadelphia Pennsylvania, USA 19140

[#]School of Pathology and Laboratory Medicine, University of Western Australia, Crawley 6009 Australia

Abstract

Cbl and Cbl-b are E3 ubiquitin ligases and adaptor proteins, which perform regulatory roles in bone remodeling. Cbl−/− mice have delayed bone development due to decreased osteoclast migration. Cbl-b−/− mice are osteopenic due to increased bone resorbing activity of osteoclasts. Unique to Cbl, but not present in Cbl-b, is tyrosine 737 in the YEAM motif, which upon phosphorylation provides a binding site for the regulatory p85 subunit of PI3K. Substitution of tyrosine 737 with phenylalanine (Y737F, CblYF/YF mice) prevents Y737 phosphorylation and abrogates the Cbl-PI3K interaction. We have previously reported that CblYF/YF mice had increased bone volume due to defective bone resorption and increased bone formation. Here we show that the lumbar vertebra from CblYF/YF mice did not have significant bone loss following ovariectomy. Our data also suggests that abrogation of Cbl-PI3K interaction in mice results in the loss of coupling between bone resorption and formation, since ovariectomized CblYF/YF mice did not show significant changes in serum levels of c-terminal telopeptide (CTX), whereas the serum levels of pro-collagen type-1 amino-terminal pro-peptide (P1NP) were decreased. In contrast, following ovariectomy, Cbl−/− and Cbl-b−/− mice showed significant bone loss in tibiae and L2 vertebrae, concomitant with increased serum CTX and P1NP levels. These data indicate that while

[1]To whom correspondence should be addressed: Archana Sanjay, asanjay@uchc.edu.

lack of Cbl or Cbl-b distinctly affects bone remodeling, only the loss of Cbl-PI3K interaction protects mice from significant bone loss following ovariectomy.

Keywords

Cbl; Cbl-b; PI3K; osteoclast; bone resorption; ovariectomy

Introduction

Bone is continuously remodeled during life due to resorption by osteoclasts and formation by osteoblasts. Perturbation of either process results in bone disease, including osteoporosis. Most commonly observed in post-menopausal women, osteoporosis is associated with rates of bone resorption by osteoclasts are greater than the ability of osteoblasts to form new bone [1]. However the molecular mechanisms involved in this process are not well understood. Acute estrogen withdrawal observed in mice following removal of the ovaries (ovariectomy, OVX) represents a model for studying the mechanism(s) of bone loss during a dynamic state of bone remodeling.

Cbl family proteins, Cbl and Cbl-b are E3-ubiquitin ligases with adaptor function that are expressed in several cell types [2]. Independent of their E3-ubiquitin ligase activity, which targets phosphorylated proteins to degradation or to vesicular trafficking, Cbl proteins also facilitate several signaling events through protein-protein binding domains [3, 4]. The absence of both Cbl and Cbl-b in mice results in embryonic lethality prior to E10.5, suggesting overlapping functions of these two family members [5]. Cbl and Cbl-b are expressed in both osteoblasts and osteoclasts. The absence of either protein in mice does not have profound effect on osteoblast differentiation or function [6, 7]. However, the loss of Cbl in mice results in delayed bone development due to decreased migration of osteoclasts [6]. Defective osteoclast migration of Cbl−/− osteoclasts has also been observed using *in vitro* migration [6, 8]. In spite of defective migration, adult Cbl−/− mice do not show an overt skeletal phenotype because of a compensatory over-expression of Cbl-b [6]. In contrast to the adult Cbl−/− mice, deletion of Cbl-b in mice results in significant bone loss due to osteoclastic hyperactivity both in vivo and in vitro [7, 9]. Overexpression of Cbl-b in Cbl-b−/− osteoclasts prevents the increase in pit formation but overexpression of Cbl did not rescue the hyperactivity of Cbl-b−/− osteoclasts [7], indicating that both proteins perform unique roles in osteoclasts.

Cbl and Cbl-b share similar structural features and domain organization. However, one major difference between Cbl and Cbl-b is the mechanism by which they interact with phosphatidylinositol-3 kinase (PI3K), a lipid kinase that is important for osteoclast differentiation, survival and function [10]. Cbl-b associates constitutively with the p85 subunit of PI3K and targets it for vesicular trafficking without altering its levels [11]. Cbl interacts with the SH2 domain of p85 subunit of PI3K upon phosphorylation of Y737 in the YEAM motif, resulting in activation of PI3K [12, 13]. Tyrosine 737 is unique to Cbl and is not present in Cbl-b. A substitution of tyrosine to phenylalanine (Y737F) prevents phosphorylation of Cbl at this site and abrogates Cbl-PI3K interaction [14]. We previously

established that mice bearing Y737F mutation (CblYF/YF mice) had increased bone volume due to decreased bone resorption and increased bone formation, suggesting that both osteoclast and osteoblast functions are affected in the absence of the Cbl-PI3K interaction [9, 15–17].

To further understand the roles of Cbl and Cbl-b in skeletal biology during dynamic conditions of bone remodeling, we performed ovariectomy, a well-established model that enhances bone turnover [18, 19]. In this report, we demonstrate that following ovariectomy both Cbl–/– and Cbl-b–/– mice suffer significant bone loss. In contrast, ovariectomized CblYF/YF mice, in which Cbl-PI3K interaction is lost, are protected from significant bone loss due to uncoupling of osteoclast and osteoblast functions. These results indicate that Cbl-mediated regulation of PI3K is required for both basal and the enhanced bone remodeling following ovariectomy and that the absence of Cbl-PI3K interaction prevents CblYF/YF mice from having significant OVX-induced bone loss.

Materials and Methods

Mice

Cbl–/–, Cbl-b–/–, CblYF/YF mice were generated as described previously [5, 20, 21]. All mice used in this study were on a mixed background of C57bl/6J x129/SvJ. All experiments were performed in compliance with Institutional Animal Care and Use Committee, Temple University, Philadelphia, PA and the University of Connecticut Health Center, Farmington, CT.

Ovariectomy

Eight-week old virgin female mice were used in OVX studies. Following anesthesia, a 2 cm incision was made on mid-dorsal surface, thereafter fallopian tubules were ligated and ovaries were excised. In SHAM mice, similar procedure was performed except ovaries were exposed but were not removed. The surgical incision was closed and mice were maintained in a pathogen-free facility. Six weeks following surgery, serum was collected for analysis. Tibiae and vertebral columns were isolated and fixed in 10% formaldehyde in PBS for further analysis. Following OVX mice did not show significant differences in body weight or tibial length. However, loss of estrogen resulted in uterine atrophy with a 10-fold decrease in uterine weight indicating successful removal of the ovaries (Supplementary Figure 1).

3D micro-computed tomography of bone samples

MicroCT analysis was performed as previously described [9, 17, 22]. An *ex vivo* microCT scanner (SkyScan 1172, Aartslaar, Belgium) was used. Scanning was performed with a source setting of 60keV/167 µA and a 0.5mm Al filter to minimize the beam hardening from the polychromatic nature of the sealed X-ray source. Scans were made with a rotation step of 0.40 degrees through 180 degrees and a pixel size of 6 µm. Tibiae were scanned from their proximal end to mid-diaphysis (1335 slices; each slice = 6 µm). After scanning, Feldkamp cone-beam reconstruction algorithm was used to reconstruct the 3D cross-sections along with addressing the ring artifact reduction and beam hardening correction. 3D

microstructural image data and structural indices were then calculated using the Skyscan CT Analyzer (CTAn) software. Using this software, cortical and trabecular bone was separated with a region of interest tool. Trabecular morphometric traits were computed from binarized images using direct 3D techniques that do not rely on prior assumptions from the underlying structures. The volume of interest for trabecular microarchitectural variables was bounded to the endocortical margin, starting 1.9 mm from the proximal tibial condyles, just distal to the growth plate, in the direction of the metaphysis, and then extending from this position for 100 slices (0.6 mm). An upper threshold of 255 and a lower threshold of 80 was used to delineate each pixel as "bone" or non-bone", and trabecular bone volume per total volume percent (BV/TV%), mean trabecular thickness (Tb.Th), mean trabecular number (Tb.N), mean trabecular separation (Tb.Sp) were computed. Morphological traits of the mid-diaphyseal cortical shell were performed at a site starting 5.5 mm from the proximal tibial condyles, and then extending from this position for 100 slices (0.6 mm). Then, cortical parameters were measured. For vertebral column, second lumbar (L2) vertebra was used and the cancellous bone from cranial to caudal end plate of trabecular region of the entire vertebral body was analyzed.

Histological and Histomorphometric analysis

To label the skeleton, mice were injected with calcein (i.p., 10 mg/kg body weight) 9 and 2 days before euthanasia. Longitudinal sections (5 μM) of tibia were used to measure the fluorochrome label and both dynamic and static histomorphometry was performed as previously described [9, 17, 22]. For histomorphometric analysis, to assess changes in bone structure and remodeling, tibial sections were measured in the proximal metaphysis below the chondro-osseous junction of the secondary spongiosa using image analysis software (BIOQUANT Osteo II, Bioquant Image Analysis Corp., Nashville, TN) as described by Parfitt et al [23]. Dynamic parameters of bone formation were obtained using unstained sections from the trabecular surface in a defined region of interest (100 μM) below the growth plate and 50 μM from the cortical bone using a 20X objective and a Nikon 800 epifluorescent microscope. Bone formation rate (BFR) was assessed by measuring single-labeled surface for single perimeter (sL.Pm), double-labeled surface (dL.Pm), and the interlabel distance in the dL.Pms. The same sections were then evaluated under bright-field after Masson's trichrome staining to determine static parameters of bone formation: bone surface (BS), and osteoblast numbers (Ob.N). The following parameters were then calculated: mineral apposition rate (MAR, mM/day), BFR (BFR/BS), and (Ob.S/BS). For the determination of osteoclast parameters including number of osteoclasts over bone perimeter (N. OC/B.Pm) and osteoclast surface/bone surface (Oc/BS), adjacent sections were subjected to TRAP and hematoxylin staining (Sigma Aldrich, St. Louis, MO).

Serum analysis of bone turnover marker and inflammatory cytokines

Six weeks following OVX, mice were kept for 6 hours without food prior to collection of blood by retro-orbital bleeding. Serum was separated and stored at −80° C until further use. Levels of CTX, P1NP, IL-1β, IL-6, TNF-α and osteopontin in serum was determined using commercial kits.

FACS analysis

Bone marrow was isolated from tibiae and femora, six weeks following ovariectomy. Following lysis of red blood cells using RBC lysis buffer (Sigma, St. Louis, MO, USA), single cell suspensions were prepared by passing the cells through 100μm Nytex mesh. Cells were stained with CD11b conjugated to FITC and F4/80 conjugated to PE (Invitrogen, Camarillo, CA) or appropriate isotype controls (BD Pharmingen, San Jose, CA) using staining medium (1X Hank's balanced salt solution containing 10mM HEPES and 2% new born calf serum). Dead cells were identified and excluded by using propidium iodide staining. FACS analysis was performed using BD FACS Calibur (Franklin Lakes, NJ).

Statistical analysis

To determine the statistical significance between different groups of mice and the effects of ovariectomy, data was analyzed by two-way ANOVA with Bonferroni Post-hoc test using Prism 5 software. A p-value of less than 0.05 was considered statistically significant.

Results

Loss of Cbl-PI3K interaction protects mice from significant bone loss following ovariectomy

Our previous studies showed that in contrast to adult Cbl−/− mice, adult mice expressing Cbl protein with a point mutation due to substitution of tyrosine 737 to phenylalanine had increased bone volume due to defective osteoclast function and increased osteoblast function [15–17, 23]. We hypothesized, that if, the ability of Cbl to interact with PI3K were one of the determining factors regulating bone remodeling, then the loss of Cbl-PI3K interaction in CblYF/YF mice would prevent significant bone loss following ovariectomy. To test this hypothesis, eight week old virgin female CblWT/WT and CblYF/YF mice were subjected to SHAM or OVX procedure and assessed for the effects of acute estrogen withdrawal on bone volume in the second lumbar vertebra (L2) and tibia at six weeks following surgery.

In agreement with previously published results [15–17], microCT analysis of L2 vertebra from CblYF/YF SHAM mice showed higher bone volume compared to CblWT/WT SHAM mice (Figure 1 A, B). In the L2 vertebra of CblWT/WT OVX mice, bone volume (BV/TV %), trabecular thickness and trabecular number decreased by 29%, 35% and 10% respectively whereas trabecular separation increased by 26% when compared to the CblWT/WT SHAM mice. In contrast, no significant changes were observed in the L2 vertebra of CblYF/YF mice following OVX (Figure 1A–E). Similar to results in the L2 vertebra, the tibial trabecular region also demonstrated statistically significant bone loss following OVX in CblWT/WT mice but not in CblYF/YF mice (Figure 2A–E). As previously reported [17], the mid-shaft cortical region of tibia showed higher bone area and cortical thickness in CblYF/YF mice compared to Cbl WT/WT. However, no significant changes in the cortical bone microarchitecture were observed as a result of OVX (Supplementary Table 1).

Acute estrogen withdrawal results in uncoupled bone resorption and bone formation in mice lacking Cbl-PI3K interaction

To evaluate the mechanism, which confers protection from significant bone loss following ovariectomy in CblYF/YF mice, serum levels of c-terminal collagen cross-links (CTX), a marker of osteoclast activity [24] and levels of pro-collagen type-1 amino-terminal pro-peptide (P1NP), a marker of osteoblast activity [24] were analyzed. Compared to CblWT/WT SHAM mice, CTX levels increased by 48% in CblWT/WT OVX mice, however, serum CTX levels were not altered in CblYF/YF mice following ovariectomy when compared to CblYF/YF SHAM mice (Figure 3A). In agreement with previously published studies [15, 17] compared to CblWT/WT SHAM mice, CblYF/YF SHAM mice demonstrated increased osteoblast activity (Figure 3B). Interestingly, as a result of estrogen withdrawal, serum P1NP levels decreased by 37% in CblYF/YF mice (Figure 3B).

Histomorphometric analysis of the tibial trabecular region showed increased bone formation (bone formation rate/bone surface) associated with increase in both osteoblasts and osteoclasts numbers in CblWT/WT mice due to OVX (Table 1). In contrast, in CblYF/YF OVX mice, while the number of osteoclasts did not change, the number of osteoblasts and the bone formation rate were significantly decreased compared to CblYF/YF SHAM mice (Table 1 and Supplementary Figure 2).

Cumulatively, these data suggest that the loss of Cbl-PI3K interaction confers protection from significant bone loss due to uncoupling of osteoclasts and osteoblasts following OVX.

Bone remodeling is accelerated in mice following ovariectomy in the absence of Cbl or Cbl-b

To determine whether protection from bone loss following OVX is unique to the loss of Cbl-PI3K interaction, bone remodeling following ovariectomy was also evaluated in mice lacking Cbl or Cbl-b. It has been previously reported that adult male Cbl−/− mice have similar bone volume to that of CblWT/WT mice [6]. Here we observed that when compared to the CblWT/WT mice, 14wk old female Cbl−/− mice (SHAM) showed higher bone volume although this difference was not statistically significant. In response to OVX, the L2 vertebra of Cbl−/− mice showed a decrease of 12%, 18% and 16% in the BV/TV%, trabecular thickness and trabecular number respectively and an increase of 20% in the trabecular separation relative to SHAM mice. This degree of bone loss was lower than the bone loss observed in the L2 vertebra of CblWT/WT mice (Figure 4A–E).

We have previously reported that the absence of Cbl-b in mice result in osteopenia due hyperactivity of osteoclasts [7, 9]. In agreement with our published report, in this study we found that SHAM operated Cbl-b−/− mice showed lower bone volume when compared to counterpart CblWT/WT mice. Upon acute estrogen withdrawal, BV/TV% decreased by 40% in Cbl-b−/− mice (Figure 4A–E). Significant bone loss was also observed in the tibial trabecular region of CblWT/WT, Cbl−/− and Cbl-b−/− mice following OVX (Figure 5A–E). But the mid-cortical region did not show significant alterations due to OVX in CblWT/WT, Cbl−/− mice (Supplementary Table. 1). Analysis of serum CTX levels showed that OVX resulted in significant increase in the osteoclast activity with the serum CTX levels increased

in CblWT/WT mice (increase of 48%), Cbl−/− (17%) and Cbl-b−/− (18%) compared to SHAM operated mice (Figure 6A). Serum levels of bone formation also changed and we found that following OVX, P1NP levels increased by 70%, 101% and 59%, in CblWT/WT, Cbl−/− and Cbl-b−/− mice respectively (Figure 6B). When compared to Cbl−/− SHAM mice histomorphometric analysis of tibiae from Cbl−/− OVX mice showed no significant differences in the mineral apposition rate, bone formation rate, and in numbers of osteoblasts or osteoclasts (Table 1 and Supplementary Figure 2). In case of Cbl-b−/− mice following ovariectomy, static or dynamic parameters of bone formation and numbers of osteoclasts and osteoblasts, could not be determined by histomorphometric analysis due to the presence of very few trabeculae in the tibiae (data not shown). However following ovariectomy, compared to SHAM Cbl-b−/− there was a significant decrease in bone area and cortical thickness in the OVX Cbl-b−/− mice (Supplementary Table. 1).

Pro-inflammatory cytokines are thought to be involved in the increased bone remodeling that occurs after estrogen withdrawal [25, 26]. Although the role of Cbl-PI3K interaction in inflammatory responses is not reported, Cbl and Cbl-b have been shown to play important roles in T cell functions [27–31]. Therefore, we examined the serum levels of IL-1β, IL-6, TNFα or osteopontin following ovariectomy in Cbl−/− and Cbl-b−/− mice. Our results show that following ovariectomy serum levels of IL1b and TNF-α increased in CblWT/WT, Cbl−/− and Cbl-b−/− mice, serum levels of IL-6 were increased in Cbl−/− mice while levels of OPN were not altered significantly in any of the genotypes compared to the respective SHAM-operated mice (Supplementary Table 2). We next examined the numbers of CD11b and F4/80 positive cells, which belong to the myeloid/macrophage lineage and are major producers of IL-1β and TNF-α [32]. Flow cytometry showed that following OVX the numbers of CD11b and F4/80 cells were increased in all genotypes tested (Supplementary Figure 3).

Discussion

This study demonstrates that the loss of Cbl-PI3K interaction due to a Cbl Y737F mutation in mice prevents significant bone loss following ovariectomy due to: (1) lack of an increase in bone remodeling due to defective osteoclast function and (2) decreased osteoblast function. Thus the resultant uncoupling between bone resorption and bone formation protects CblYF/YF mice from significant bone loss due to ovariectomy.

Absence of Cbl-PI3K interaction prevented significant bone loss in both L2 vertebra and the tibial trabecular region. While the L2 vertebrae were completely protected from bone loss following ovariectomy, in the tibial trabecular region, some bone loss was observed by micro CT analysis, which was not statistically significant (Figure 1 and 2). Under basal condition, tibiae from CblYF/YF mice have increased cortical bone volume [17], and no significant changes were observed in the bone formation parameters of cortical bone in SHAM and OVX CblYF/YF mice (Supplementary Table 1). Thus, the differences in the degree of bone loss observed in L2 vertebrae, tibial trabecular and cortical regions is probably due to differences in the rate of bone remodeling in different anatomical sites as a result of the absence of Cbl-PI3K interaction. Similar differences in bone volume in different bones are also reported for other mouse models [33, 34].

Our results also demonstrate that although both CblYF/YF mice and Cbl−/− mice lack Cbl-PI3K interaction, only CblYF/YF mice are protected from estrogen-withdrawal induced bone loss. This observation suggests the following possibilities: (1) the increase in Cbl-b that occurs in Cbl−/− mice may be sufficient to preserve the effects of OVX on bone that are seen in WT mice. However, because the increase in Cbl-b is not seen in YF mice [15] these animals do not lose bone mass after OVX. (2) While Cbl−/− osteoclasts have decreased migration, the osteoclast resorptive activity in adult Cbl−/− mice is comparable to CblWT/WT mice [7, 9], and the osteoclast activity increases upon estrogen withdrawal (Figure 6A). In contrast, the osteoclast activity in CblYF/YF mice is reduced [9, 15] and not altered as a result of OVX (Figure 3A). (3) Finally, while histomorphometric and biochemical markers of bone formation are significantly decreased in OVX CblYF/YF mice, they are not altered to a similar degree in Cbl−/− mice (Table 1, Figure 3B). Together these observations suggest that the uncoupling between bone resorption and formation is more pronounced in the absence of Cbl-PI3K interaction than in the absence of Cbl protein.

Cbl and Cbl-b have been demonstrated to perform distinct roles in bone remodeling [35]. Cbl plays an important role in osteoclast migration [6, 8], while Cbl-b plays an important role to negatively regulate bone resorption by osteoclasts [7]. The opposite effects on the skeletal phenotype in the absence of Cbl and Cbl-b proteins is likely related to their interactions with distinct proteins in osteoclasts and/or osteoblasts. In this study we found that upon estrogen withdrawal the extent of bone loss and the markers levels of bone resorption and formation markers in the absence of Cbl and Cbl-b proteins were comparable (Figure 4–6A) suggesting that these two closely related proteins may be able to compensate for the absence of each other during the dynamic condition of bone remodeling.

While the function of T and B cells are not reported to alter in CblYF/YF mice, absence of Cbl or Cbl-b in mice is known to modulate T cell immune responses [27, 28, 30, 31]. It has been hypothesized that T cells play a pivotal role in the mechanism of estrogen induced bone loss [25, 26]. Our results show that the degree of bone loss and the increase in osteoclast function were mitigated in the absence of Cbl. However, these observations are not directly related to ovariectomy-induced inflammatory response, since the levels of IL-1β, TNFα, IL-6 in OVX Cbl−/− mice were significantly higher compared to OVX CblWT/WT mice (Supplementary Table 2). Following ovariectomy the number of myeloid/macrophage cells increased more in CblWT/WT and Cbl-b−/− mice than in Cbl−/− mice. Taken together, these results indicate that myeloid cells in Cbl$^{−/−}$ OVX mice are more responsive to the effects of ovariectomy, although there was a relatively smaller increase in their number. No substantial change in the numbers or function of osteoblasts is seen in OVX Cbl−/− mice when compared to SHAM Cbl−/−mice; although the direct effect of the loss of estrogen on osteoblast survival and function in Cbl−/− mice remains to be investigated. Recent work has suggested that in addition to having a major role in osteoclast migration, Cbl also negatively regulates osteoblast differentiation through ubiquitylation and degradation of FGFR2 and PDGFRα [36]. Cbl also regulates osteoblast survival via regulating the surface expression of α5 integrin [37] and by regulating PI3K/AKT signaling [38].

We have previously demonstrated that Cbl-b negatively regulates osteoclast function [7]. Others have reported that Cbl-b regulates IGF (Insulin-like growth factor) signaling and contributes to osteoblast proliferation [39]. In this report we found that in contrast to Cbl–/– mice, ovariectomy-induced bone loss in Cbl-b–/– mice was more pronounced than it was in CblWT/WT mice (Figure 4B, 5B). An effect that was probably due to increased osteoclast function (Figure 6A, B). Thus both in Cbl–/– or Cbl-b–/– mice, increased osteoclast activity was associated with increased osteoblast function, but the net result was estrogen withdrawal-induced bone loss.

In response to ovariectomy two major differences in CblYF/YF mice were observed when compared to CblWT/WT, Cbl–/– or Cbl-b–/– mice. First, in contrast to Cbl–/– and Cbl-b–/– mice, which showed increased CTX levels, CblYF/YF mice did not show any change in this parameter. Second, in contrast to all genotypes, which had increased serum P1NP levels, estrogen withdrawal in CblYF/YF mice resulted in a significant decrease in serum P1NP levels. It is possible that the decreased osteoclast function in CblYF/YF mice after OVX was due to a lack of Cbl-PI3K interaction, which in turn abrogated the signal(s) needed for increased osteoblast proliferation, differentiation and function. Recent work from several groups has suggested that both functional and non-functional osteoclasts can regulate osteoblast differentiation and function [40–42]. Thus the loss of coupling of osteoclast and osteoblasts functions provides an explanation for the absence of significant bone loss in CblYF/YF mice following ovariectomy.

Interestingly, the absence of Cbl, Cbl-b or Cbl-PI3K interaction resulted in much lower, albeit not statistically significant cortical bone loss in tibia suggesting that the bone remodeling events in Cbl mutant mice are more relevant to the trabecular regions than the cortical regions. Hence, understanding the contribution of osteocytes, which are more abundant in cortical than in trabecular bone, is important and is a subject of future studies.

In conclusion, we provide evidence that the Cbl-PI3K interaction is required for significant bone loss due to acute estrogen withdrawal following ovariectomy in mice. Selective modulation of Cbl-PI3K interaction might provide a valuable tool to understand the molecular mechanisms of bone remodeling, which result in bone loss due to osteoporosis in postmenopausal women.

Supplementary Material

Refer to Web version on PubMed Central for supplementary material.

Acknowledgments

References

1. Turner RT. Mice, estrogen, and postmenopausal osteoporosis. Journal of bone and mineral research : the official journal of the American Society for Bone and Mineral Research. 1999; 14:187–191.

2. Swaminathan G, Tsygankov AY. The Cbl family proteins: ring leaders in regulation of cell signaling. Journal of cellular physiology. 2006; 209:21–43. [PubMed: 16741904]

3. Thien CB, Langdon WY. c-Cbl and Cbl-b ubiquitin ligases: substrate diversity and the negative regulation of signalling responses. Biochem J. 2005; 391:153–166. [PubMed: 16212556]

4. Thien CBF, Langdon WY. Cbl: many adaptations to regulate protein tyrosine kinases. Nat. Rev. Mol. Cell. Biol. 2001; 2:294–305. [PubMed: 11283727]

5. Naramura M, Jang I-K, Kole H, Huang F, Haines D, Gu H. c-Cbl and Cbl-b regulate T cell responsiveness by promoting ligand-induced TCR down-modulation. Nature immunology. 2002; 3:1192–1199. [PubMed: 12415267]

6. Chiusaroli R, Sanjay A, Henriksen K, Engsig MT, Horne WC, Gu H, Baron R. Deletion of the gene encoding c-Cbl alters the ability of osteoclasts to migrate, delaying resorption and ossification of cartilage during the development of long bones. Dev Biol. 2003; 261:537–547. [PubMed: 14499658]

7. Nakajima A, Sanjay A, Chiusaroli R, Adapala NS, Neff L, Itzsteink C, Horne WC, Baron R. Loss of Cbl-b increases osteoclast bone-resorbing activity and induces osteopenia. Journal of bone and mineral research : the official journal of the American Society for Bone and Mineral Research. 2009; 24:1162–1172.

8. Sanjay A, Houghton A, Neff L, DiDomenico E, Bardelay C, Antoine E, Levy J, Gailit J, Bowtell D, Horne WC, Baron R. Cbl associates with Pyk2 and Src to regulate Src kinase activity, alpha(v)beta(3) integrin-mediated signaling, cell adhesion, and osteoclast motility. J Cell Biol. 2001; 152:181–195. [PubMed: 11149930]

9. Adapala NS, Barbe MF, Tsygankov A, Lorenzo J, Sanjay A. Loss of Cbl-PI3K interaction enhances osteoclast survival due to p21-Ras mediated PI3K activation independent of Cbl-b. Journal of cellular biochemistry. 2014

10. Shinohara M, Nakamura M, Masuda H, Hirose J, Kadono Y, Iwasawa M, Nagase Y, Ueki K, Kadowaki T, Sasaki T, Kato S, Nakamura H, Tanaka S, Takayanagi H. Class IA phosphatidylinositol 3-kinase regulates osteoclastic bone resorption through protein kinase B-mediated vesicle transport. Journal of bone and mineral research : the official journal of the American Society for Bone and Mineral Research. 2012; 27:2464–2475.

11. Fang D, Liu YC. Proteolysis-independent regulation of PI3K by Cbl-b-mediated ubiquitination in T cells. Nat Immunol. 2001; 2:870–875. [PubMed: 11526404]

12. Feshchenko EA, Shore SK, Tsygankov AY. Tyrosine phosphorylation of C-Cbl facilitates adhesion and spreading while suppressing anchorage-independent growth of V-Abl-transformed NIH3T3 fibroblasts. Oncogene. 1999; 18:3703–3715. [PubMed: 10391678]

13. Ueno H, Sasaki K, Honda H, Nakamoto T, Yamagata T, Miyagawa K, Mitani K, Yazaki Y, Hirai H. c-Cbl is tyrosine-phosphorylated by interleukin-4 and enhances mitogenic and survival signals of interleukin-4 receptor by linking with the phosphatidylinositol 3'-kinase pathway. Blood. 1998; 91:46–53. [PubMed: 9414268]

14. Hunter S, Burton EA, Wu SC, Anderson SM. Fyn associates with Cbl and phosphorylates tyrosine 731 in Cbl, a binding site for phosphatidylinositol 3-kinase. The Journal of biological chemistry. 1999; 274:2097–2106. [PubMed: 9890970]

15. Adapala NS, Barbe MF, Langdon WY, Nakamura MC, Tsygankov AY, Sanjay A. The loss of Cbl-phosphatidylinositol 3-kinase interaction perturbs RANKL-mediated signaling, inhibiting bone resorption and promoting osteoclast survival. The Journal of biological chemistry. 2010; 285:36745–36758. [PubMed: 20851882]

16. Adapala NS, Barbe MF, Langdon WY, Tsygankov AY, Sanjay A. Cbl-phosphatidylinositol 3 kinase interaction differentially regulates macrophage colony-stimulating factor-mediated osteoclast survival and cytoskeletal reorganization. Annals of the New York Academy of Sciences. 2010; 1192:376–384. [PubMed: 20392263]

17. Brennan T, Adapala NS, Barbe MF, Yingling V, Sanjay A. Abrogation of Cbl-PI3K interaction increases bone formation and osteoblast proliferation. Calcified tissue international. 2011; 89:396–410. [PubMed: 21952831]

18. Li JY, Adams J, Calvi LM, Lane TF, Weitzmann MN, Pacifici R. Ovariectomy expands murine short-term hemopoietic stem cell function through T cell expressed CD40L and Wnt10B. Blood. 2013; 122:2346–2357. [PubMed: 23954891]

19. Zhao H, Kitaura H, Sands MS, Ross FP, Teitelbaum SL, Novack DV. Critical role of beta3 integrin in experimental postmenopausal osteoporosis. Journal of bone and mineral research : the official journal of the American Society for Bone and Mineral Research. 2005; 20:2116–2123.

20. Molero JC, Turner N, Thien CB, Langdon WY, James DE, Cooney GJ. Genetic ablation of the c-Cbl ubiquitin ligase domain results in increased energy expenditure and improved insulin action. Diabetes. 2006; 55:3411–3417. [PubMed: 17130487]

21. Naramura M, Kole HK, Hu RJ, Gu H. Altered thymic positive selection and intracellular signals in Cbl- deficient mice. Proc Natl Acad Sci U S A. 1998; 95:15547–15552. [PubMed: 9861006]

22. Back SH, Adapala NS, Barbe MF, Carpino NC, Tsygankov AY, Sanjay A. TULA-2, a novel histidine phosphatase, regulates bone remodeling by modulating osteoclast function. Cellular and molecular life sciences : CMLS. 2012

23. Parfitt AM, Drezner MK, Glorieux FH, Kanis JA, Malluche H, Meunier PJ, Ott SM, Recker RR. Bone histomorphometry: standardization of nomenclature, symbols, and units. Report of the ASBMR Histomorphometry Nomenclature Committee. J. Bone Miner. Res. 1987; 2:595–610. [PubMed: 3455637]

24. Ebeling PR, Peterson JM, Riggs BL. Utility of type I procollagen propeptide assays for assessing abnormalities in metabolic bone diseases. Journal of bone and mineral research : the official journal of the American Society for Bone and Mineral Research. 1992; 7:1243–1250.

25. Weitzmann MN, Pacifici R. The role of T lymphocytes in bone metabolism. Immunological reviews. 2005; 208:154–168. [PubMed: 16313347]

26. Weitzmann MN, Pacifici R. Estrogen deficiency and bone loss: an inflammatory tale. The Journal of clinical investigation. 2006; 116:1186–1194. [PubMed: 16670759]

27. Bachmaier K, Krawczyk C, Kozieradzki I, Kong YY, Sasaki T, Oliveira-dos-Santos A, Mariathasan S, Bouchard D, Wakeham A, Itie A, Le J, Ohashi PS, Sarosi I, Nishina H, Lipkowitz S, Penninger JM. Negative regulation of lymphocyte activation and autoimmunity by the molecular adaptor Cbl-b. Nature. 2000; 403:211–216. [PubMed: 10646608]

28. Thien CB, Blystad FD, Zhan Y, Lew AM, Voigt V, Andoniou CE, Langdon WY. Loss of c-Cbl RING finger function results in high-intensity TCR signaling and thymic deletion. The EMBO journal. 2005; 24:3807–3819. [PubMed: 16211006]

29. Thien CB, Dagger SA, Steer JH, Koentgen F, Jansen ES, Scott CL, Langdon WY. c-Cbl promotes TCR-induced thymocyte apoptosis by activating the PI3K/Akt pathway. J Biol Chem. 2010; 285:10969–10981. [PubMed: 20133944]

30. Thien CB, Scaife RM, Papadimitriou JM, Murphy MA, Bowtell DD, Langdon WY. A mouse with a loss-of-function mutation in the c-Cbl TKB domain shows perturbed thymocyte signaling without enhancing the activity of the ZAP-70 tyrosine kinase. J Exp Med. 2003; 197:503–513. [PubMed: 12591907]

31. Thien CBF, Bowtell DDL, Langdon WY. Perturbed regulation of ZAP-70 and sustained tyrosine phosphorylation of LAT and SLP-76 in c-Cbl-deficient thymocytes. J Immunol. 1999; 162:7133–7139. [PubMed: 10358158]

32. Pacifici R. Estrogen, cytokines, and pathogenesis of postmenopausal osteoporosis. Journal of bone and mineral research : the official journal of the American Society for Bone and Mineral Research. 1996; 11:1043–1051.

33. Anginot A, Dacquin R, Mazzorana M, Jurdic P. Lymphocytes and the Dap12 adaptor are key regulators of osteoclast activation associated with gonadal failure. PloS one. 2007; 2:e585. [PubMed: 17611620]

34. Wu Y, Torchia J, Yao W, Lane NE, Lanier LL, Nakamura MC, Humphrey MB. Bone microenvironment specific roles of ITAM adapter signaling during bone remodeling induced by acute estrogen-deficiency. PloS one. 2007; 2:e586. [PubMed: 17611621]

35. Horne WC, Sanjay A, Bruzzaniti A, Baron R. The role(s) of Src kinase and Cbl proteins in the regulation of osteoclast differentiation and function. Immunological reviews. 2005; 208:106–125. [PubMed: 16313344]

36. Severe N, Miraoui H, Marie PJ. The Casitas B lineage lymphoma (Cbl) mutant G306E enhances osteogenic differentiation in human mesenchymal stromal cells in part by decreased Cbl-mediated platelet-derived growth factor receptor alpha and fibroblast growth factor receptor 2 ubiquitination. The Journal of biological chemistry. 2011; 286:24443–24450. [PubMed: 21596750]

37. Kaabeche K, Guenou H, Bouvard D, Didelot N, Listrat A, Marie PJ. Cbl-mediated ubiquitination of alpha5 integrin subunit mediates fibronectin-dependent osteoblast detachment and apoptosis induced by FGFR2 activation. J Cell Sci. 2005; 118:1223–1232. [PubMed: 15728256]

38. Dufour C, Guenou H, Kaabeche K, Bouvard D, Sanjay A, Marie PJ. FGFR2-Cbl interaction in lipid rafts triggers attenuation of PI3K/Akt signaling and osteoblast survival. Bone. 2008; 42:1032–1039. [PubMed: 18374639]

39. Suzue N, Nikawa T, Onishi Y, Yamada C, Hirasaka K, Ogawa T, Furochi H, Kosaka H, Ishidoh K, Gu H, Takeda S, Ishimaru N, Hayashi Y, Yamamoto H, Kishi K, Yasui N. Ubiquitin ligase Cbl-b downregulates bone formation through suppression of IGF-I signaling in osteoblasts during denervation. J Bone Miner Res. 2006; 21:722–734. [PubMed: 16734387]

40. Lotinun S, Kiviranta R, Matsubara T, Alzate JA, Neff L, Luth A, Koskivirta I, Kleuser B, Vacher J, Vuorio E, Horne WC, Baron R. Osteoclast-specific cathepsin K deletion stimulates S1P-dependent bone formation. The Journal of clinical investigation. 2013; 123:666–681. [PubMed: 23321671]

41. Takeshita S, Namba N, Zhao JJ, Jiang Y, Genant HK, Silva MJ, Brodt MD, Helgason CD, Kalesnikoff J, Rauh MJ, Humphries RK, Krystal G, Teitelbaum SL, Ross FP. SHIP-deficient mice are severely osteoporotic due to increased numbers of hyper-resorptive osteoclasts. Nature medicine. 2002; 8:943–949.

42. Walker EC, McGregor NE, Poulton IJ, Pompolo S, Allan EH, Quinn JM, Gillespie MT, Martin TJ, Sims NA. Cardiotrophin-1 is an osteoclast-derived stimulus of bone formation required for normal bone remodeling. Journal of bone and mineral research : the official journal of the American Society for Bone and Mineral Research. 2008; 23:2025–2032.

Highlights

Cbl family of protein plays distinct roles during normal and pathological bone remodeling

Mice lacking Cbl-PI3K interaction due to tyrosine to phenylalanine mutation (Y737F, CblYF/YF mice) are protected from significant bone loss.

Upon ovariectomy CblYF/YF mice demonstrate uncoupling of osteoclast and osteoblast functions, preventing bone loss up on acute estrogen withdrawal.
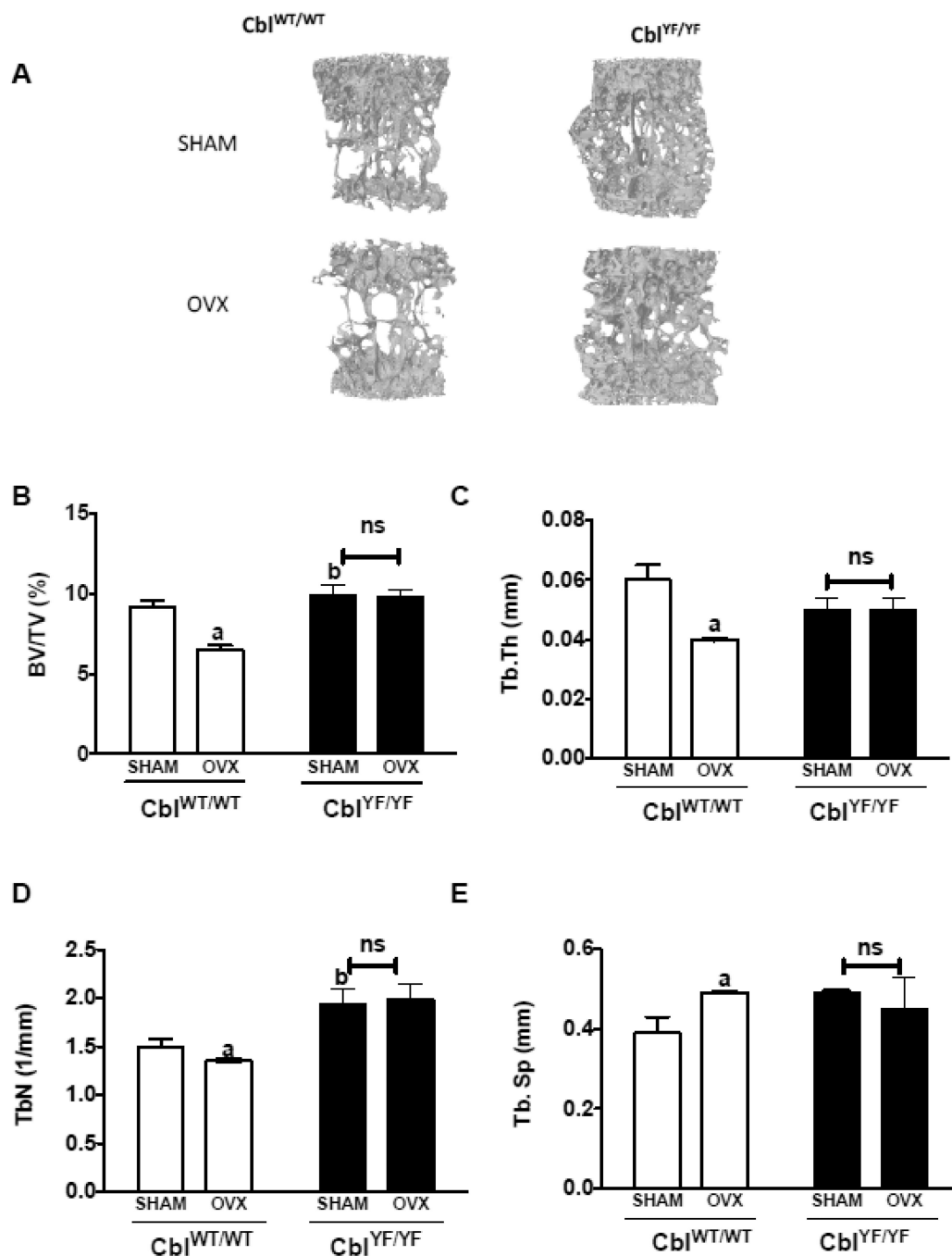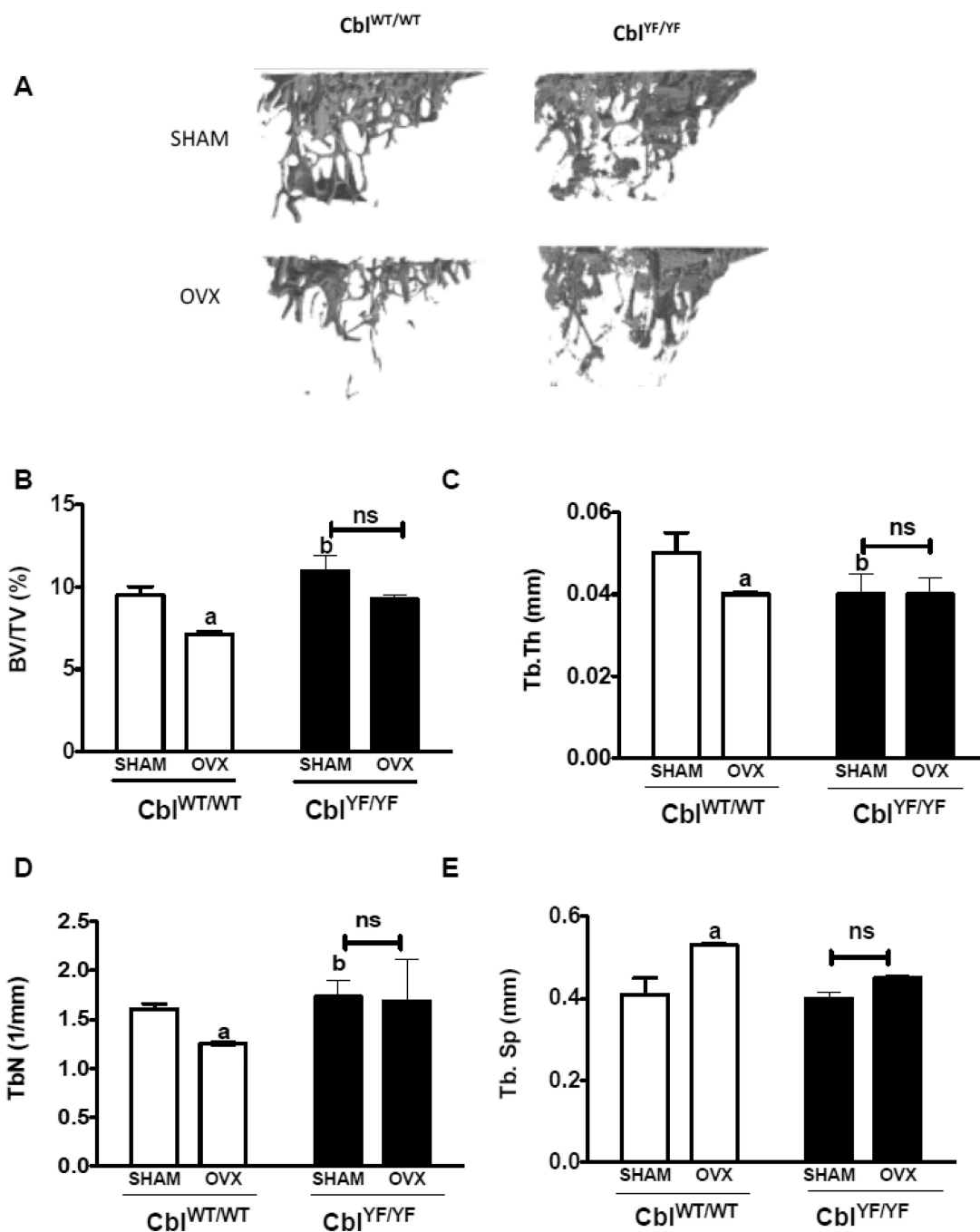
Figure 1. Trabecular bone parameters in the second lumbar vertebra of mice lacking Cbl-PI3K interaction following ovariectomy
A. Three dimensional (3D) μCT images of second lumbar vertebra (L2) showing bone volume in CblWT/WT and CblYF/YF mice. L2 Vertebra of SHAM operated mice (n=6) are shown in the top panel and ovariectomized (OVX) mice (n=6) in the bottom panel. **B.** BV/TV% (percentage of Bone volume/Trabecular volume) is in CblWT/WT (white bars) and CblYF/YF (black bars) mice. **C.** Tb. Th (Trabecular thickness in mm) **D.** Tb.N (Trabecular Number) **E.** Tb. Sp (Trabecular Separation). Data are presented as mean ± SD

from indicated number of mice and compared with SHAM. p<0.05 was considered statistically significant as compared to respective controls using two way ANOVA with Bonferroni post-test. a, CblWT/WT SHAM vs OVX; b, CblWT/WT SHAM vs CblYF/YF SHAM. ns, not significant.

Figure 2. Trabecular bone parameters in the tibia of mice lacking Cbl-PI3K interaction following ovariectomy
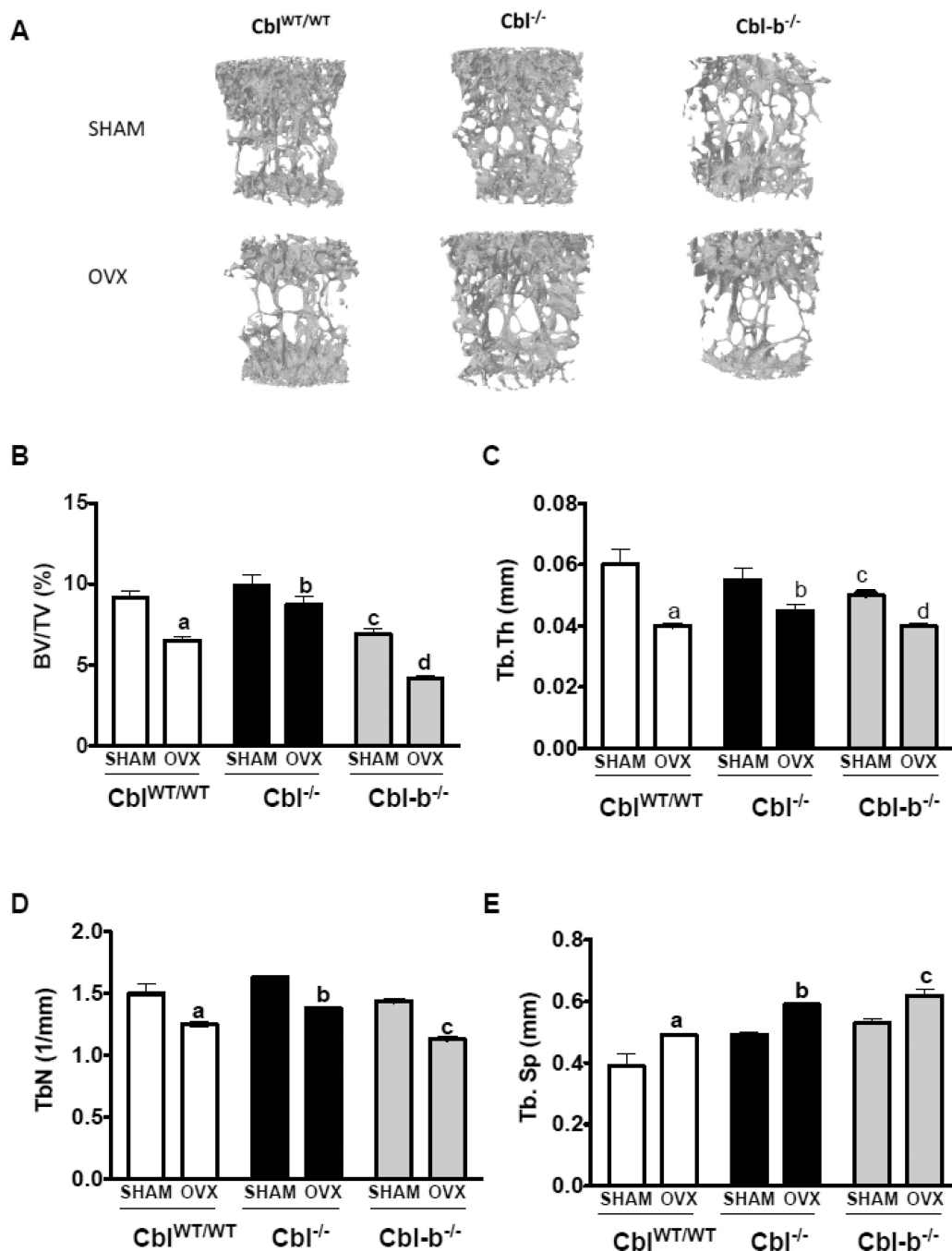
A. Three dimensional (3D) μCT images of tibial trabecular region showing bone volume in CblWT/WT and CblYF/YF mice. Tibiae of SHAM operated mice (n=6) are shown in the top panel and ovariectomized (OVX) mice (n=6) in the bottom panel. **B.** BV/TV% (Percentage of Bone volume/Trabecular volume) in CblWT/WT (white bars) and CblYF/YF (black bars) mice. **C.** Tb. Th (Trabecular thickness in mm) **D.** Tb. N (Trabecular Number) **E.** Tb. Sp (Trabecular Separation). Data are presented as mean ± SD from indicated number of

mice and compared with SHAM. p<0.05 was considered statistically significant as compared to respective controls using two way ANOVA with Bonferroni post-test a, CblWT/WT SHAM vs OVX; b, CblWT/WT SHAM vs CblYF/YF SHAM. ns, not significant.
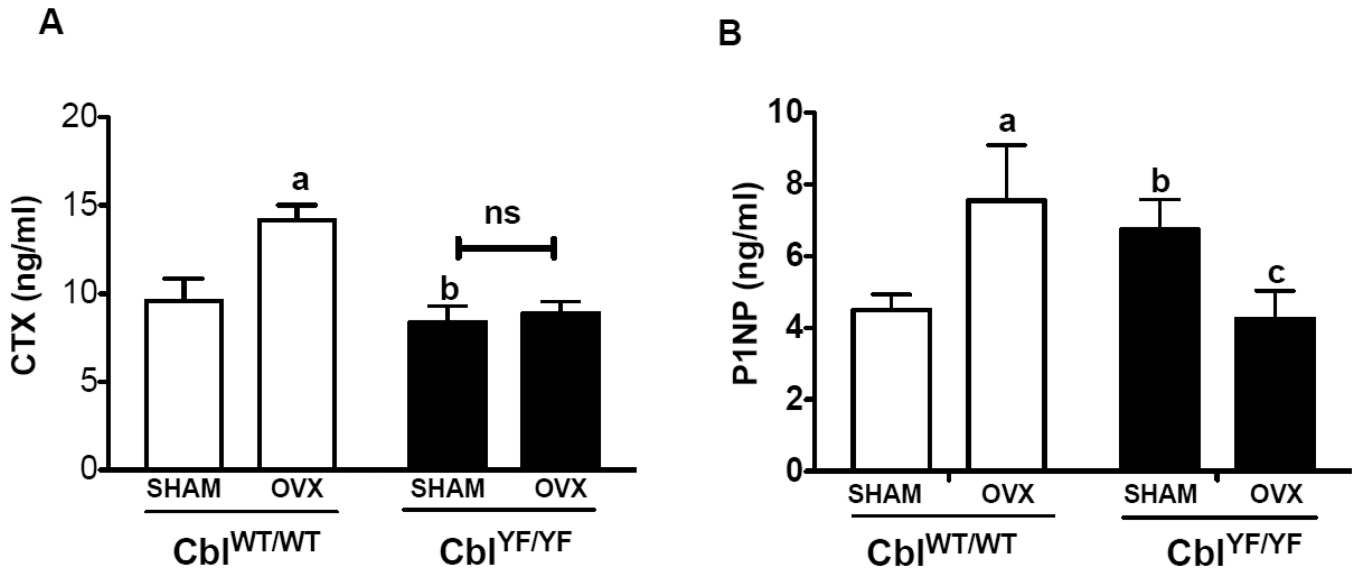
Figure 3. Effect of ovariectomy on the osteoclast and osteoblast functions in mice lacking Cbl-PI3K interaction

Serum levels of c-terminal telopeptide (CTX) reflective of *in vivo* osteoclast activity and pro-collagen type 1 amino-terminal pro-peptide (P1NP) were determined. Serum was collected from SHAM operated mice (n=6) and ovariectomized (OVX) mice (n=6) six weeks following surgery, and the levels CTX and P1NP were determined using ELISA. **A.** Serum levels of CTX in CblWT/WT (white bars) and CblYF/YF (black bars) are presented. **B.** Serum levels of P1NP are shown. Data are presented as mean ± SD from indicated number of mice and compared with SHAM. p<0.05 was considered statistically significant as compared to respective controls using two way ANOVA with Bonferroni post-test. a, CblWT/WT SHAM vs OVX; b, CblWT/WT SHAM vs CblYF/YF SHAM; c, CblYF/YF SHAM vs OVX. ns, not significant.
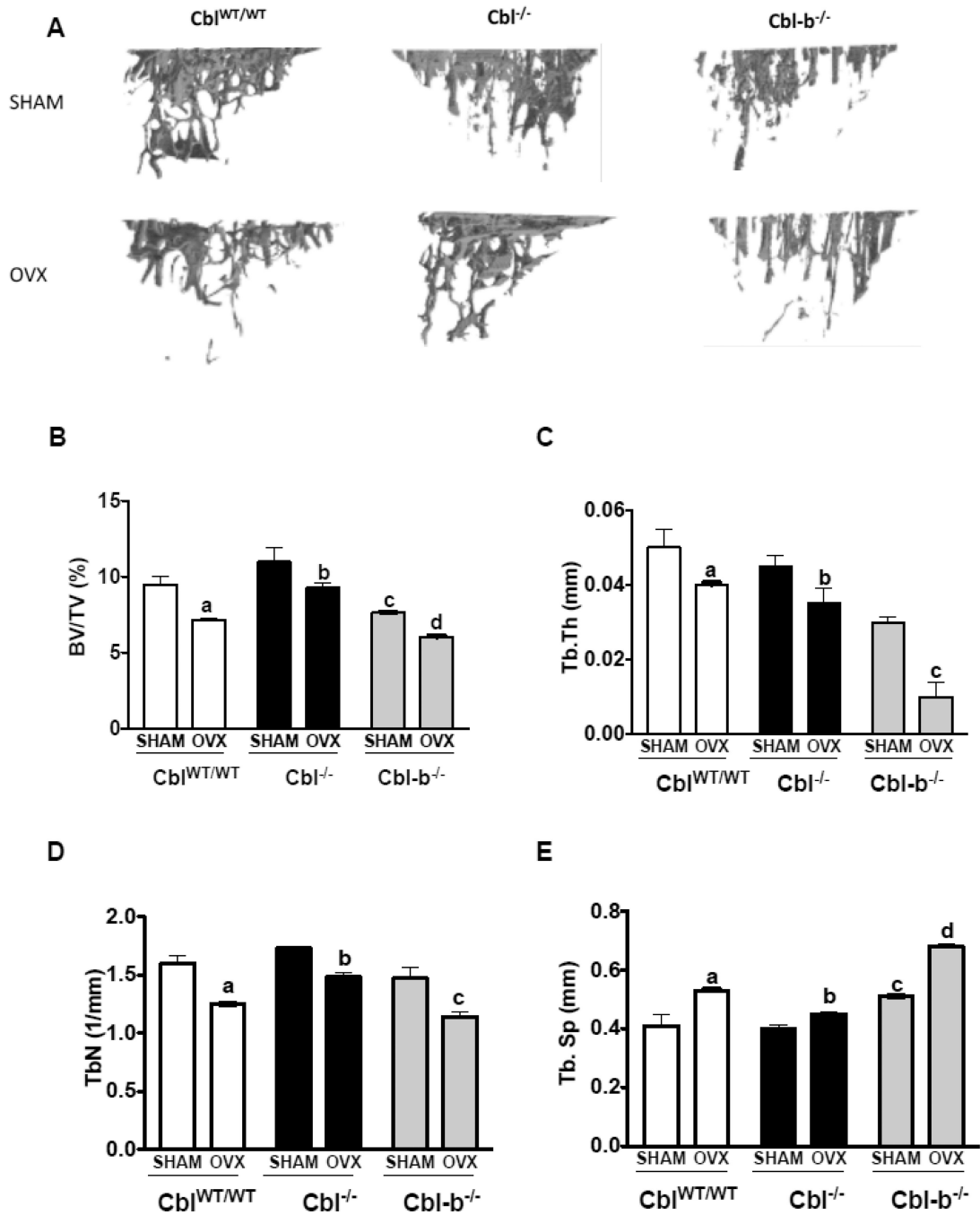
Figure 4. Trabecular bone parameters in the second lumbar vertebra of mice lacking Cbl or Cbl-b following ovariectomy

A. Three dimensional (3D) μCT images of second lumbar vertebra (L2) showing decreased bone volume due to ovariectomy (OVX). Vertebrae of SHAM operated mice (n=6) are shown in the top panel and ovariectomized mice (n=6) in the bottom panel. **B.** BV/TV% (percentage of Bone volume/Trabecular volume) in CblWT/WT (white bars), Cbl–/− (black bars) and Cbl-b–/− (grey bars). **C.** Tb. Th (Trabecular thickness in mm). **D.** Tb. N (Trabecular Number). **E.** Tb. Sp (Trabecular Separation). Data are presented as mean ± SD

from indicated number of mice and compared with SHAM. p<0.05 was considered statistically significant as compared to respective controls using two way ANOVA with Bonferroni post-test. Panels B, C: a, CblWT/WT SHAM vs OVX; b, Cbl–/– SHAM vs OVX; c, CblWT/WT SHAM vs Cbl-b–/– SHAM; d, Cbl-b–/– SHAM vs OVX. Panels D, E: c, Cbl-b–/– SHAM vs OVX.

Figure 5. Trabecular bone parameters in the tibia of mice lacking Cbl or Cbl-b following ovariectomy

A. Three dimensional (3D) μCT images of proximal tibial trabecular region showing bone loss due to ovariectomy (OVX). Tibiae of SHAM operated mice (n=6) are shown in the top panel and ovariectomized mice (n=6) in the bottom panel. **B.** BV/TV% (percentage of Bone volume/Trabecular volume) in CblWT/WT (white bars), Cbl–/– (black bars) and Cbl-b–/– (grey bars). **C.** Tb. Th (Trabecular thickness in mm). **D.** Tb. N (Trabecular Number). **E.** Tb. Sp (Trabecular Separation). Data are presented as mean ± SD from indicated number of

mice and compared with SHAM. p<0.05 was considered statistically significant as compared to respective controls using two way ANOVA with Bonferroni post-test. Panels B, E: a, CblWT/WT SHAM vs OVX; b, Cbl–/– SHAM vs OVX; c, CblWT/WT SHAM vs Cbl-b–/– SHAM; d, Cbl-b–/– SHAM vs OVX. Panels C, D: c, Cbl-b–/– SHAM vs OVX.
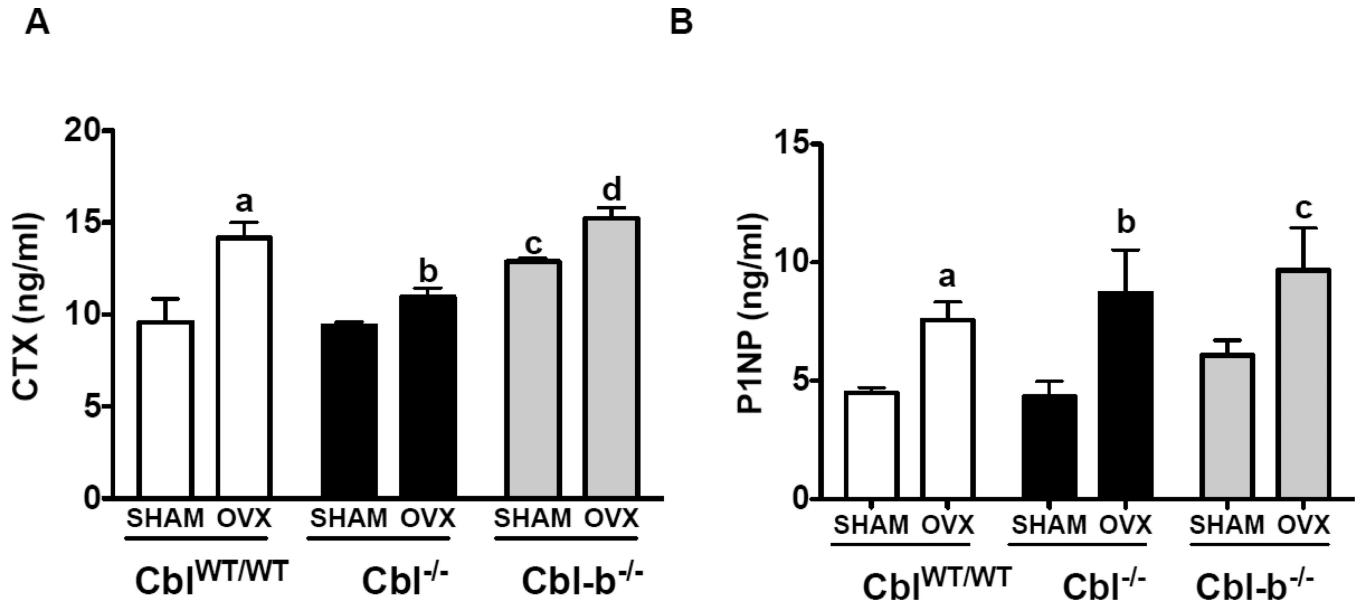
Figure 6. Effect of ovariectomy on the osteoclast and osteoblast functions in mice lacking Cbl or Cbl-b

Serum levels of c-terminal telopeptide (CTX) reflective of *in vivo* osteoclast activity and pro-collagen type 1 amino-terminal propeptide (P1NP) were determined. Serum was collected from SHAM operated mice (n=6) and ovariectomized (OVX) mice (n=6) six weeks following surgery, and the levels CTX and P1NP were determined using ELISA. **A.** Serum levels of CTX in CblWT/WT (white bars), Cbl–/– (black bars) and Cbl-b–/– (grey bars) are presented. **B.** Serum levels of P1NP are shown. Data are presented as mean ± SD from indicated number of mice and compared with SHAM. p<0.05 was considered statistically significant as compared to respective controls using two way ANOVA with Bonferroni post-test Panel A: a, CblWT/WT SHAM vs OVX; b, Cbl–/– SHAM vs OVX; c, CblWT/WT SHAM vs Cbl-b–/– SHAM; d, Cbl-b–/– SHAM vs OVX. Panel B: c, Cbl-b–/– SHAM vs OVX.

Table 1

Histomorphometric analysis of tibial trabecular region

Bone parameters of the trabecular region of tibia of SHAM operated and ovariectomized mice (OVX) was determined by histomorphometric analysis. Mineral apposition rate (MAR), Bone formation rate over bone surface (BFR/BS), Percentage of osteoblast surface over bone surface (Ob.S/BS%), Number of osteoclasts over bone perimeter (N. OC/B.Pm) and Osteoclast surface over bone surface (Oc.S/BS) as determined by histomorphometry are shown. Values shown are mean ± SD from Cbl$^{WT/WT}$: SHAM n=5, OVX n=5; Cbl$^{YF/YF}$: SHAM n=5, OVX n=5 Cbl−/−: SHAM n=5, OVX n=6.

Genotype		MAR (μm/d)	BFR/BS (μm³/μm²/d)	Ob.S/BS (%)	N. OC/B.Pm (No./mm)	Oc.S/BS (%)
Cbl$^{WT/WT}$	SHAM	0.72 ± 0.22	0.19 ± 0.04	12.31 ± 2.28	2.96 ± 0.42	5.02 ± 1.63
	OVX	1.04 ± 0.36	0.38 ± 0.16*	18.24 ± 2.90*	5.33 ± 0.91*	9.25 ± 2.21*
Cbl$^{YF/YF}$	SHAM	0.85 ± 0.17	0.21 ± 0.08	15.55 ± 0.90	5.38 ± 0.31	10.7 ± 1.39
	OVX	0.64 ± 0.07*	0.10 ± 0.06*	11.41 ± 2.43*	4.84 ± 0.81	8.33 ± 1.33
Cbl$^{−/−}$	SHAM	0.71 ± 0.08	0.23 ± 0.03	10.87 ± 0.43	3.75 ± 0.21	5.38 ± 0.31
	OVX	0.95 ± 0.19	0.38 ± 0.29	10.74 ± 0.57	4.20 ± 0.68	6.84 ± 0.81

*
p<0.05 compared to SHAM mice was considered statistically significant as compared to respective controls using two way ANOVA with Tukey's post-hoc test.